JOURNAL OF MATERIALS SCIENCE 26 (1991) 6473–6478

Deformation behaviour of NiTi shape memory alloys in bending

M. THIER, A. MICK, D. DRESCHER, C. BOURAUEL
Department of Orthodontics, University of Bonn, Welschnonnenstrasse 17, D-5300 Bonn 1, Germany

The deformation behaviour of memory alloys is exactly that of a linear-elastic and ideal-plastic material. A short report on the description of bending deformation of such a material in continuum mechanics is given. According to the parameters of geometry and material the bending deformation of NiTi memory alloy is first illustrated and later characterized by its parameters and limitations.

1. Introduction

Unusual deformation behaviour is one of the characteristics of shape memory alloys. On reaching a specific stress level, the deformation proceeds while the applied force remains constant (Fig. 1). The basic crystallographic mechanism of this kind of deformation is the twinning deformation of martensite and the stress-induced formation of martensite [1]. Both deformation mechanisms may lead to the memory effect. A stress-induced formation of martensite in a thermodynamic stable parent phase is called pseudoelasticity.

Up to now the NiTi alloy has been the most important shape memory material. A lot of applications in technics and medicine are introduced [2–4]. Investigations have been carried out and a great amount of information on deformation behaviour is available, especially on the tensile properties [5–7]. Nevertheless, very little information exists about the memory characteristics in other stress states. Only torsional properties of pseudoelastic NiTi were studied [8] but no information is available about the deformation characteristics in bending. For example the correction of tooth position is a bending application of pseudoelastic NiTi alloy [9]. To realize and to improve such applications in medicine or in technics it is necessary to describe the deformation of such bending memory elements.

The aim of this paper is to give a guideline on the characteristics of deformation behaviour of NiTi shape memory material in bending. Continuum mechanics offers a proper theory to describe pure bending deformation [10]. The shape memory alloy is indeed an ideal example to study the pure bending of a linear-elastic ideal-plastic material. The subject of this paper is, given the geometry and material constants, to ascertain the bending deformation characteristics of the memory material as well as the realization of a defined memory bending application where the geometry and material constants have to be found out.

2. Theory of pure bending in linear-elastic and ideal-plastic materials

A short report on the theoretical background will be given here. More detailed information on this subject is available in the literature [11, 12].

2.1. Determination of the stress–strain distribution

A square shaped beam (Fig. 2) which is deformed by a pure moment M_y is the basis of the following explanations. To get the strain distribution in the bended state a characteristic part of the beam is drawn out (Fig. 3). The strain $\varepsilon(z)$ is defined as

$$\varepsilon(z) = \frac{l_1 - l_0}{l_0} \tag{1}$$

where l_0 is the origin length and l_1 the length in the bended state. The length of the neutral fibre is l_0 and that of $l_1(z)$ for $-h/2 \leqslant z \leqslant h/2$ is

$$l_1(z) = \frac{R_z + z}{R_z} l_0 \tag{2}$$

which can be taken out of Fig. 2. The strain distribution $\varepsilon(z)$ for $-h/2 \leqslant z \leqslant h/2$ is now given by Equation 2 in Equation 1

$$\varepsilon(z) = \frac{z}{R_z} \tag{3}$$

i.e. a linear function of $\varepsilon(z)$ describes the strain distribution for every bending radius R_z.

To characterize the stress distribution the deformation process has to be divided into periods of different deformation mechanisms (Fig. 4). The first period is determined by pure linear-elastic deformation behaviour up to that point where the stress σ at $z = \pm h/2$ becomes σ_f (flow stress). The second period is that of mixed deformation behaviour, i.e. linear-elastic deformation as well as ideal-plastic deformation.

The stress distribution in the first period for $0 \leqslant z \leqslant \pm h/2$ is

$$\sigma(z) = E\frac{z}{R_z} \tag{4}$$

In the second period the stress distribution is for

0022–2461/91 $03.00 + .12

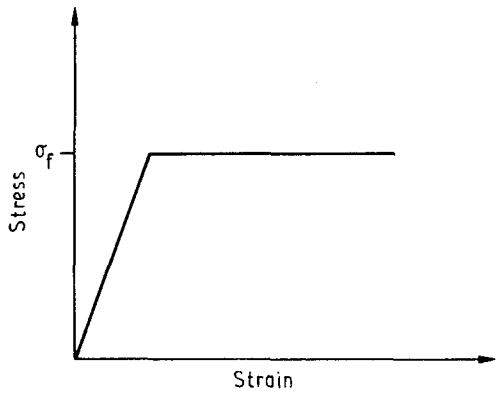

Figure 1 Deformation characteristic of a shape memory alloy; at a constant stress level σ_f the deformation proceeds by twinning deformation or stress induced formation of martensite.

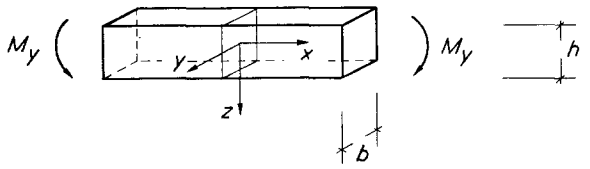

Figure 2 Geometry parameters of the beam to describe the deformation of NiTi in pure bending.

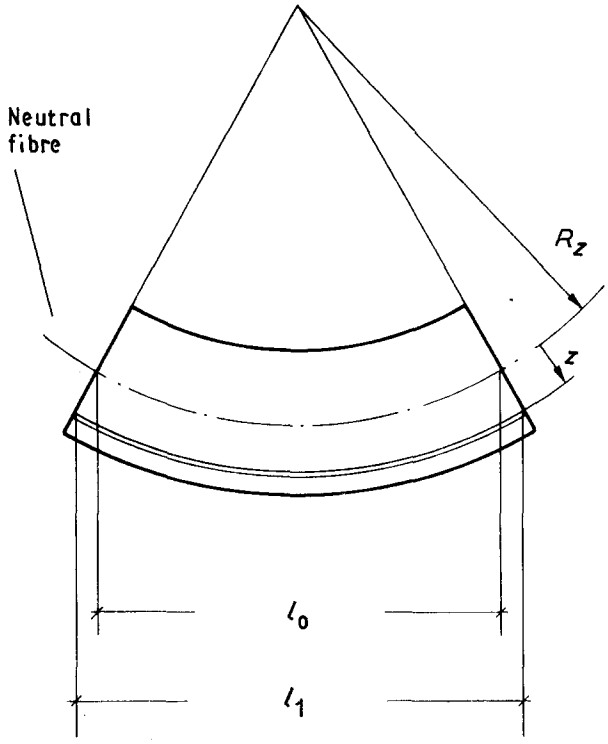

Figure 3 Part of the beam in bended configuration to find out the strain distribution.

$0 \leqslant z \leqslant z_f$, i.e. the linear elastic deformation behaviour is again given by Equation 4; for $z_f \leqslant z \leqslant \pm h/2$ $\sigma(z)$ is constant

$$\sigma(z) = \sigma_f \tag{5}$$

The upper limit of deformation is determined by the strain at $\varepsilon(z = \pm h/2)$ thus the requirements of continuum mechanics and NiTi memory material behaviour this limit is set on $\varepsilon(\pm h/2) = 6\%$.

2.2. Linear-elastic deformation and upper limit

The bending moment M_y and the sum of the internal forces are in balance, i.e. the moment M_y can be expressed as

$$M_y = \int_A z\sigma(z)\mathrm{d}A \tag{6}$$

The stress distribution of the first period is given in Equation 4. The linear-elastic deformation characteristic is described by the moment M_y as a function of $1/R_z$ the reciprocal bending radius

$$M_y = \frac{Ebh^3}{12}\frac{1}{R_z} \tag{7}$$

The limit of the linear-elastic behaviour is determined by $\sigma(z = \pm h/2) = \sigma_f$; from Equation 4 follows the minimum reciprocal elastic bending radius

$$\frac{1}{R_{zE}} = \frac{2\sigma_f}{Eh} \tag{8}$$

and the maximum elastic moment, Equation 7 in Equation 8

$$M_{yE} = \frac{bh^2}{6}\sigma_f \tag{9}$$

The limit of the linear-elastic behaviour $M_{yE} = f(1/R_{zE})$ according to the geometry and the material constants will be discussed in Sections 3 and 4.1.

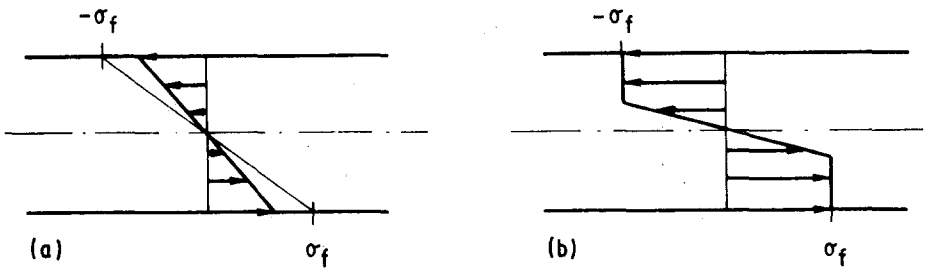

Figure 4 Periods of different deformation mechanism characterized by elastic deformation respectively deformation of martensite or stress induced formation of martensite. (a) period 1, (b) period 2.

2.3. Mixed deformation and upper limit

Again the moment M_y is given by the sum of the internal forces; the important difference is that there are two deformation mechanisms present now. Each part is taken by itself, so the bending moment is

$$M_y = \int_{A_E} z\sigma(z)\mathrm{d}A + \int_{A_P} z\sigma(z)\mathrm{d}A \qquad (10)$$

The stress distribution for the linear-elastic section (A_E) and that for the ideal-plastic section (A_P) is given in Equations 4 and 5. In the second period the deformation characteristic $M_y = f(1/R_z)$ becomes

$$\frac{M_y}{M_{yE}} = \frac{3}{2}\left[1 - \frac{1}{3}\left(\frac{R_z}{R_{zE}}\right)^2\right] \qquad (11)$$

The upper limit of deformation is determined by the strain $\varepsilon(z)$. The limitation was set on $\varepsilon(z) \leqslant 6\%$. The characteristics of deformation behaviour in the second period depending on the geometry and material constants will be discussed in the following chapters.

3. Illustration of deformation behaviour

The pure bending of a linear-elastic ideal-plastic material described above will now be taken to illustrate (Section 3) and later exactly characterize (Section 4) the deformation behaviour of a NiTi shape memory material in bending.

The deformation characteristic is perfectly described in Equations 7 and 11. The parameters of geometry are the height h and the ratio width to height b/h of the beam. The material constants are Young's modulus, E, and the flow stress, σ_f. This study was intended to deal with the bending deformation behaviour of the NiTi shape memory alloys so that Young's modulus was set to $E \approx 50\,000$ MPa.

Just to illustrate the influence of the geometry parameters h and b/h and that of the material constant σ_f, one of the parameters was varied in the following order

h(mm) : 0.4 0.6 0.8 (Fig. 5a)

b/h : 0.5 1.0 1.5 (Fig. 5b)

σ_f (MPa) : 150 300 450 (Fig. 5c)

while the others were set to

h (mm) : 0.4

b/h : 1.0

σ_f (MPa) : 300

The plots were realized by the help of a computer programme. In Fig. 5a a strong dependence of the elastic and memory-like deformation behaviour on the height of the beam is documented. Enlarging the height will produce a strong increase in stiffness of the elastic period and a similar increase of the maximum bending moment when the deformation becomes memory-like.

The influence on stiffness and maximum bending moment seems to be much smaller when the ratio width to height b/h of the beam is varied (Fig. 5b).

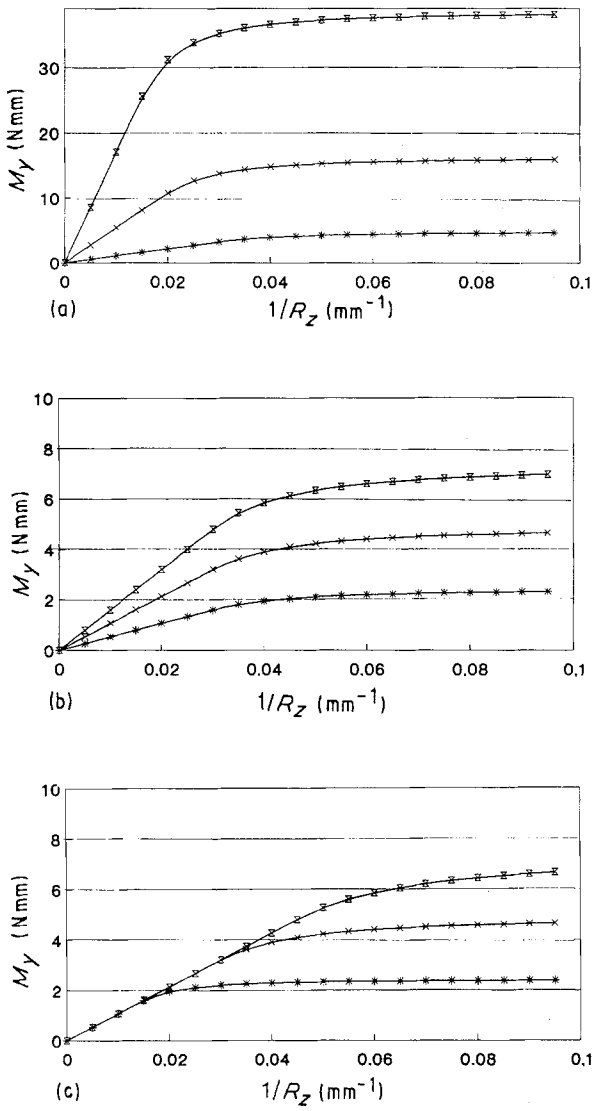

Figure 5 Illustration of NiTi bending deformation behaviour by computer programme plots. The parameters varied are (a) beam height (* 0.4 mm, × 0.6 mm, X 0.8 mm $b/h = 1$ flow stress 300 MPa), (b) ratio b/h (* 0.5, × 1.0, X 1.5 height = 0.4 mm, flow stress 300 MPa) and (c) flow stress (* 150 MPa, × 300 MPa, X 450 MPa, height = 0.4 mm, $b/h = 1$).

There is a small change in stiffness similar to the change in the maximum bending moment.

Different bending deformation characteristic becomes visible when the flow stress σ_f is varied (Fig. 5c). There is no influence on the stiffness and a similar influence on the maximum bending moment as in Fig. 5b.

4. Bending deformation characteristic of NiTi alloys

4.1. Upper limit of linear-elastic deformation

One point of interest in the bending deformation characteristic of NiTi shape memory alloys is the dependence of the bending yield point on the geometry of the beam and the flow stress of the alloy. The deformation mechanism changes from linear-elastic deformation to the twinning deformation of martensite respectively to the stress induced formation of martensite.

The variations of all the possible yield points ($M_{yE} = f(1/R_{zE})$) for the parameters of Fig. 5a–c is

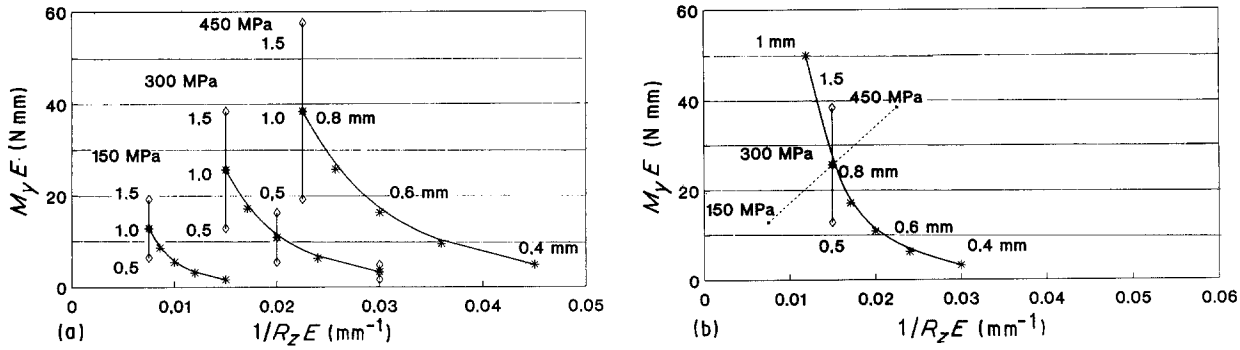

Figure 6 Influence of beam height (*), ratio b/h (◇) and flow stress (- - - -) on the elastic yield point in bending deformation of NiTi memory alloy.

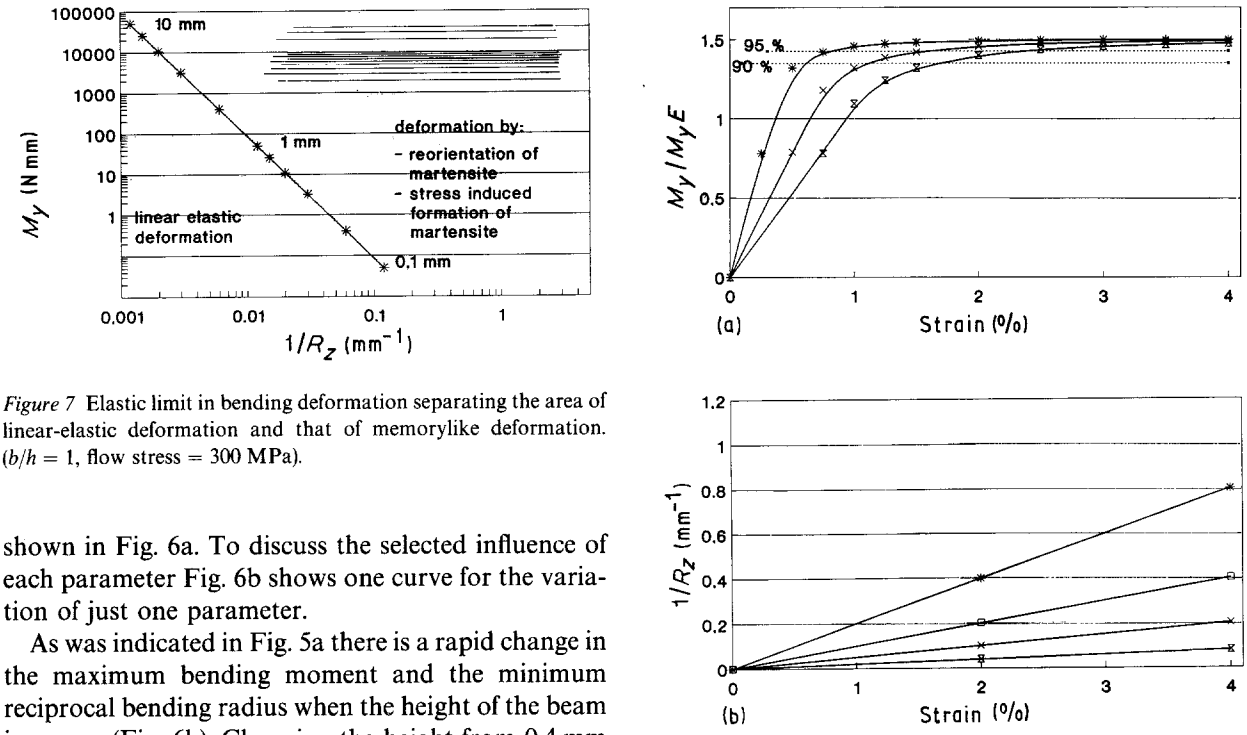

Figure 7 Elastic limit in bending deformation separating the area of linear-elastic deformation and that of memorylike deformation. (b/h = 1, flow stress = 300 MPa).

Figure 8 Characteristic of (a) moment (flow stress: * 150 MPa, × 300 MPa, X 450 MPa; .... M_y = 90(95)% $M_{y\,max}$) and (b) reciprocal radius against strain at the border of the beam ($z = \pm h/2$) (height: * 0.1 mm, □ 0.2 mm, ×0.4 mm, X 1.0 mm).

shown in Fig. 6a. To discuss the selected influence of each parameter Fig. 6b shows one curve for the variation of just one parameter.

As was indicated in Fig. 5a there is a rapid change in the maximum bending moment and the minimum reciprocal bending radius when the height of the beam increases (Fig. 6b). Changing the height from 0.4 mm to 1.0 mm produces an increase in the maximum moment from 4 N mm up to 50 N mm while the minimum reciprocal bending radius changes from 0.03 to 0.012 mm^{-1}. The ratio width to height $b/h = 1$ and the flow stress $\sigma_f = 300$ MPa.

In the next curve of Fig. 6b the ratio width to height b/h is varied. The height $h = 0.8$ mm and the flow stress $\sigma_f = 300$ MPa. There is no influence of the ratio b/h on the reciprocal bending radius. The influence on the maximum elastic bending moment may be described here by an increase in the bending moment M_{yE} from 26 to 38 N mm when the ratio b/h is changed from 1.0 to 1.5.

The last parameter is a change in the flow stress σ_f. There is the same influence on the bending moment and on the reciprocal bending radius. An increase in flow stress σ_f from 300 to 450 MPa will produce an increase in the bending moment from 26 to 38 N mm (same as in ratio b/h) while the reciprocal bending radius changes from 0.015 to 0.0225 mm^{-1}.

The yield point for a beam height between 0.1 mm and 10 mm ($b/h = 1$; $\sigma_f = 300$ MPa) is shown in Fig. 7. On the left-hand side of the curve there is linear-elastic deformation behaviour while on the right-hand side there is the twinning deformation of martensite or rather the stress induced formation of martensite. Using this diagram it is now easy to determine what maximum elastic moment can be realized when the height of the beam is chosen and secondly what minimum reciprocal elastic bending radius is achieved. A change in the beam height from 1 to 4 mm for example will result in an increase of the maximum elastic bending moment M_{yE} from 50 to 3000 N mm while the reciprocal elastic bending radius is reduced from 0.01 to 0.003 mm^{-1} (minimum elastic bending radius: 100 to 333 mm).

4.2. Characteristics of bending for twinning deformation of martensite and stress induced formation of martensite

Due to its limiting character the strain $\varepsilon(z = \pm h/2)$ is an important factor in the application of memory alloys in bending. In Fig. 8a and b the development

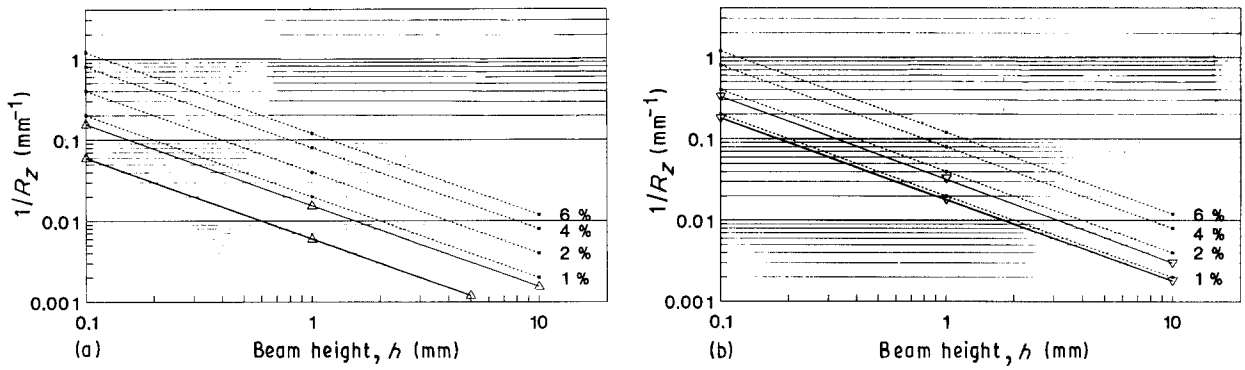

Figure 9 Description of useful strain in bending deformation for NiTi memory alloys with different flow stress levels. (a) △ 95% max, 150 MPa; △ $1/R_{zE}$ 150 MPa. (b) ▽ 90% max, 450 MPa, ▽ $1/R_{zE}$, 450 MPa.

of M_y/M_{yE} and $1/R_z$ is described as a function of $\varepsilon(z = \pm h/2)$.

The ratio of M_y/M_{yE} is a function of the strain $\varepsilon(\pm h/2)$ and the flow stress σ_f (Fig. 8a). Depending on the flow stress σ_f, i.e. the material, there is an important difference in the deformation characteristic. To describe the useful strain that is available for a NiTi bending application a 90% limit ($M_y = 0.9M_{y\max}$) is introduced. The increase in flow stress σ_f from 150 to 450 MPa produces a reduction in the useful strain from $\varepsilon_{150} = 3.4\%$ to $\varepsilon_{450} = 2.2\%$ (max. strain 4%). To get a high workability for memory alloys in bending the flow stress σ_f has to be chosen as low as possible.

The reciprocal bending moment is a function of the strain $\varepsilon(\pm h/2)$ and the height of the beam (Fig. 8b). The increase of the height will produce an enormous reduction of the reciprocal bending radius. For example ($\varepsilon = 4\%$) an increase in beam height from 0.1 to 0.4 mm will reduce the maximum reciprocal bending radius $1/R_z$ from 0.8 to 0.2 mm^{-1} (minimum bending radius from 1.25 to 5 mm). The minimum bending radius achieved for a NiTi bending application is limited by the height of the beam used.

For a beam height between 0.1 and 10 mm the characteristics and limitations of the reciprocal bending radius are shown in Fig. 9a and b. The reciprocal bending radius is set in relation to the strain $\varepsilon(\pm h/2)$. The development of the reciprocal bending radius is presented for NiTi memory alloys with 150 and 450 MPa flow stress. According to the flow stress σ_f (determination of useful strain) the characteristic limit $M_y = 90(95)\%\ M_{y\max}$ should be chosen separately (see Fig. 8a).

In Fig. 9a and b a description of the development of the reciprocal bending radius is given. One example (Fig. 9a) is a beam height of 1 mm, a NiTi alloy with a flow stress of 150 MPa and the characteristic limit (determination of useful stress) chosen to $M_y = 0.95M_{y\max}$ (see Fig. 8a). In Fig. 9a it could be seen that the elastic limit $1/R_{zE}$ and the 95% limit ($M_y = 0.95M_{y\max}$) characterizing the start of deformation by useful strain are placed well below the 1% strain $\varepsilon(\pm h/2)$ limit. The further change in reciprocal bending radius from $\varepsilon(\pm h/2) = 1\%$ to $\varepsilon(\pm h/2) = 6\%$ can be used for bending application of that memory alloy. In addition to that the absolute value of the reciprocal bending radius (i.e. bending radius) for the elastic limit, the starting point of useful deformation and the maximum value are given. For this example $1/R_{zE} = 0.006\ mm^{-1}$, $1/R_{z95} = 0.015\ mm^{-1}$ and $1/R_{z\max} = 0.12\ mm^{-1}$ i.e. $R_{zE} = 167$ mm, $R_{z95} = 67$ mm, $R_{z\max} = 8$ mm.

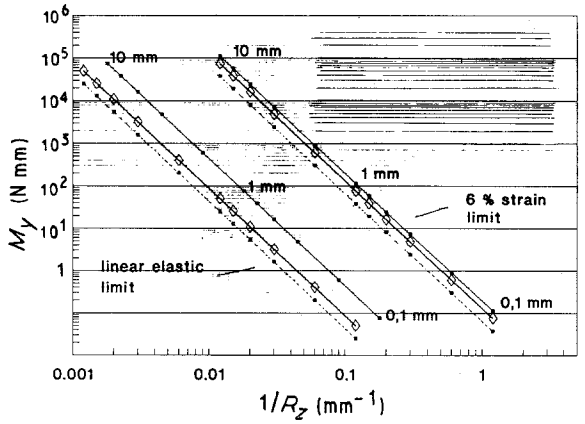

Figure 10 The influence of beam height, ratio b/h (---0.5, 300 MPa; ◇ 1.0, 300 MPa; ■ 1.0, 450 MPa) and flow stress on the elastic and maximum limit in bending deformation.

In Fig. 9a and b it is not only possible to take an alloy (parameter: flow stress σ_f), a certain beam height, get the development (limits) of the bending radius and search for an application. In practical application of memory in bending it will be right the other way; take the bending radius (R_{zE}, $R_{z90/95}$, $R_{z\max}$) you need and determine the parameters of geometry and material for realization (Fig. 9a and b). In addition characteristics of the absolute value of the maximum bending moment $M_{y\max}$ may be determined in Fig. 4a and b and Fig. 6a.

4.3. Variation of elastic and maximum limit

To characterize the possible applications of NiTi memory alloy in bending a deformation diagram was built up that summarizes the parameters discussed up to now. The area of twinning deformation of martensite and the stress induced formation of martensite

is bordered by the elastic limit on the left-hand side and by the maximum strain limit ($\varepsilon = 6\%$) on the right-hand side. The broadening or shortening of this area of bending memory is characterized by a change in the following parameters

beam height : 0.1–10 mm

ratio b/h : 0.5 1.0

flow stress σ_f : 300 MPa, 450 MPa

There is an enormous influence of the beam height h on the elastic as well as on the maximum limit. The ratio width to height b/h will only influence the bending moment of the elastic (M_{yE}) and the maximum (M_{ymax}) limit while the elastic and minimum bending radius (R_{zE}, $R_{z\,min}$) remain constant. A change in the flow stress σ_f influences the bending radius (R_{zE}) as well as the bending moment (M_{yE}) of the elastic limit; the flow stress σ_f only changes the absolute value of the moment (M_{ymax}) of the maximum limit while the minimum bending radius $R_{z\,min}$ remains constant.

5. Conclusions

The bending deformation of NiTi memory alloys reveals its own characteristics and limitations of deformation behaviour. It seems to be useful to take the geometry parameters and the material constants and to describe the bending deformation by the continuum mechanics, by the pure bending of linear-elastic and ideal-plastic material.

A description of NiTi bending deformation as was shown here, offers two important alternatives. It will give you a guideline in the first place to obtain information about what is achievable in memory bending with the material at your disposal and in the second place what material and what geometry is necessary for a memory bending application still to be realized.

Acknowledgements

The authors wish to thank the German Research Foundation DR 191 for project support.

References

1. L. DELAEY, R. V. KRISHNAN, H. TAS and H. WARLIMONT, *J. Mater. Sci.* **9** (1974) 1521.
2. D. STÖCKEL, in "The Martensitic Transformation in Science and Technology", edited by E. Hornbogen and N. Jost (DGM, Oberursel, 1989) pp. 223–230.
3. G. VON SALIS-SOGLIO, *Z. Orthoph.* **127** (1989) 191.
4. F. MIURA, M. MOGI, Y. OHURA, H. HAMANAKA, *Amer. J. Orthod. Dentofac. Orthop.* **90** (1986) 1.
5. S. MIYASAKI, Y. OHMI, K. OTSUKA and Y. SUZUKI, **C4** (1982) 255.
6. T. SABURI, M. YOSHIDA and S. NENNO, *Scripta Metall.* **18** (1984) 363.
7. G. B. STACHOWIAK and P. G. McCORMICK, *ibid.* **21** (1987) 403.
8. P. H. ADLER, W. YU, A. R. PELTON, R. ZADNO, T. W. DUERIG and R. BARRESI, *ibid.* **24** (1990) 943.
9. F. MIURA, M. MOGI, Y. OHURA and M. KARIBE, *Amer. J. Orthod. Dentofac. Orthop.* **94** (1988) 89.
10. T. LEHMANN, "Elemente der Mechanik II: Elastostatik" (Vieweg, Braunschweig, 1975) pp. 323.
11. R. HILL, "The mathematical theory of plasticity" (Oxford at the Clarendon Press, Oxford, 1950) pp. 79–81.
12. C. R. CALLADINE, "Engineering Plasticity" (Pergamon, New York, 1969) p. 55–92.

Received 15 June 1990
and accepted 31 January 1991